Accepted Manuscript

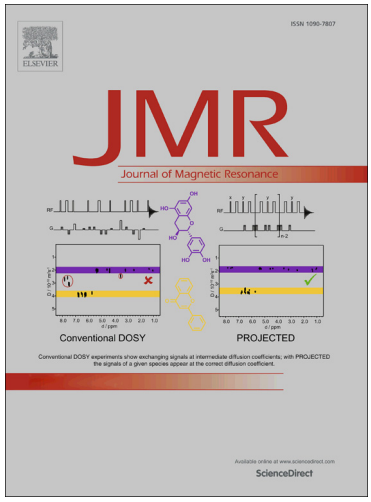

The determination of pair distance distribution by double electron-electron resonance: Regularization by the length of distance discretization with Monte Carlo calculations

Sergei A. Dzuba

PII: S1090-7807(16)30077-5
DOI: http://dx.doi.org/10.1016/j.jmr.2016.06.001
Reference: YJMRE 5882

To appear in: *Journal of Magnetic Resonance*

Received Date: 11 March 2016
Revised Date: 26 May 2016
Accepted Date: 1 June 2016

Please cite this article as: S.A. Dzuba, The determination of pair distance distribution by double electron-electron resonance: Regularization by the length of distance discretization with Monte Carlo calculations, *Journal of Magnetic Resonance* (2016), doi: http://dx.doi.org/10.1016/j.jmr.2016.06.001

Highlighted Revision copy (It the same MS as the revised version, only the parts are highlighted in which severe changes were made or new text was added). Note that all Figures are changed and 1 more Figure is added.

The determination of pair distance distribution by double electron-electron resonance: regularization by the length of distance discretization with Monte Carlo calculations

Sergei A. Dzuba

Institute of Chemical Kinetics and Combustion, RAS, Novosibirsk 630090, Russian Federation, and

Novosibirsk State University, Novosibirsk 630090, Russian Federation

Abstract

Pulsed double electron-electron resonance technique (DEER, or PELDOR) is applied to study conformations and aggregation of peptides, proteins, nucleic acids, and other macromolecules. For a pair of spin labels, experimental data allows for determination of their distance distribution function, $P(r)$. $P(r)$ is derived as a solution of a first-kind Fredholm integral equation, which is an ill-posed problem. Here, we suggest regularization by the increasing of distance discretization length, to its upper limit where numerical integration still provides agreement with experiment. This upper limit is found to be well above the lower limit for which the solution instability appears because of the ill-posed nature of the problem; so the solution indeed can be regularized in this way. For solving the integral equation, a Monte Carlo trials of $P(r)$ functions is employed. It has an obvious advantage of the fulfillment of the non-negativity constrain for $P(r)$. The approach is checked for model distance distributions and for experimental data taken from literature for doubly spin-labeled DNA and peptide antibiotics. For the case of overlapping broad and narrow distributions, "selective" regularization can be employed in which

the effective regularization length may be different for different distance ranges. The method could serve as a useful complement for the traditional approaches basing on Tikhonov regularization.

E-mail: dzuba@kinetics.nsc.ru

Key words: DEER, PELDOR, spin label, Fredholm integral equation, peptide antibiotics, DNA

Highlights

- Regularization can be achieved by increasing the distance discretization length
- The Monte Carlo search of solution converges satisfactorily fast
- The method could serve as a useful complement to the traditional approaches

1. Introduction

Pulsed double electron-electron resonance technique (DEER, also known as PELDOR) [1,2] allows measurement of distances between paramagnetic centers ranging between 1.5 and 8 nm. Distance distributions obtained from PELDOR data provide access to conformational flexibility of biomolecules (peptides, proteins, nucleic acids). Some recent applications of the technique are summarized in reviews [3-10].

Most often, these studies are aimed on deriving information on the pair distance distribution function, $P(r)$, between two spin labels attached to a biomolecule. From mathematical point of view, $P(r)$ is obtained as a solution of a first-kind Fredholm integral equation, which is an ill-posed problem. Different approaches have been employed to solve this equation [11-19]; most of them use Tikhonov regularization to stabilize the solution. These approaches allow also determination of the total number of spins in the nanoobject under study (so not only pairs of spin labels can be investigated) and the distribution of the nanoobjects in space. The most commonly employed approach utilizes the DeerAnalysis2006 software [18].

However, because of the ill-posed nature of the problem, solving of integral equation is prone for artifacts, especially when signal-to-noise ratio is not good [16,17]. Therefore development of alternative approaches is of general interest.

Here, we present an approach in which regularization of the solution is attained by increasing the discretization length, up to the threshold where numerical calculation of the integral still provides an agreement with the experimental data. Near this threshold result of the numerical integration is expected to be sensitive to deviation of the solution, so it must be stabilized. As in this approach the number N of distance points r_i in which $P(r_i)$ is sampled is not high, the integral equation can be solved by Monte Carlo trials for different distribution functions $P(r_i)$, with selection the function providing the best agreement with experimental data. In this approach, the constrain of non-negativity of $P(r_i)$ values is fulfilled automatically. (Note that maximum entropy regularization approach [17] also allows fulfillment of the non-negativity

constrain). First application of this approach was reported in [20], here it is developed and analyzed in detail.

At first look, the number of Monte Carlo trials must be extremely large because it is searching minimum in *N*-dimensional space. However the contribution of different distances when solving the integral equation is essentially non-equivalent because of the singularity of kernel of the integral equation, and therefore the number of trials may be drastically reduced.

We neglect here the possible complications arising in real PELDOR measurements such as the orientation selectivity [3-10], and the effects induced by overlapping of excitation and detection pulses [21]. These complications can be considered in the same way as in other approaches.

2. Theoretical Background

For doubly spin-labeled molecules, PELDOR time traces $V(T)$ depend on two contributions: the intramolecular one, $V_{INTRA}(T)$, arising from interactions between two labels in the molecule, and the intermolecular one, $V_{INTER}(T)$, arising from interactions between labels in different molecules. These two contributions are assumed to be independent so that $V(T)$ is a product:

$$V(T) = V_{INTRA}(T)V_{INTER}(T). \quad (1)$$

The $V_{INTER}(T)$ contribution can be obtained from experiments on mono-labeled molecules or it may be assessed from asymptotical $V(T)$ behavior at large T so the $V_{INTRA}(T)$ contribution can be normally refined from experimental data.

The theory [3-10, 21] predicts that

$$V_{INTRA}(T) = V_{INTRA}(0)(1-\lambda(1-f(T)),$$

where factor λ is determined by the parameters of the pumping pulse, and

$$f(T) = \int_0^{\pi/2} \sin\theta d\theta \int_0^{\infty} \cos(\frac{g_1 g_2 \mu_B^2}{\hbar} \frac{1}{r^3}(1-3\cos^2\theta)T))P(r)dr, \quad (2)$$

where r is the distance between the two spin labels, g_1 and g_2 are the g-factors for spin labels 1 and 2, θ is the angle between the applied magnetic field and the vector connecting the labels. The distance distribution function $P(r)$ between labels in the molecule is assumed to be normalized:

$$\int_0^\infty P(r)dr = 1 \tag{3}$$

(so making $f(0) = 1$ in Eq. (2)).

Eq. (2) is a first-kind Fredholm integral equation over $P(r)$. It could be solved if $f(T)$ is known. The latter can be derived from the experimentally obtained $V_{INTRA}(T)$ after its transformation into a normalized form:

$$V_N(T) = \frac{V_{INTRA}(T) - V_{INTRA}(\infty)}{V_{INTRA}(0) - V_{INTRA}(\infty)}, \tag{4}$$

with the subsequent suggestion that $V_N(T) = f(T)$.

Fourier transform of Eq. (2), denoted here as $F(\nu)$, may be presented as

$$F(\nu) = \int_0^\infty K(\nu, r)P(r)dr, \tag{5}$$

where

$$K(\nu, r) = 2\int_0^\infty \cos(2\pi\nu T)dT \int_0^{\pi/2} \sin\theta d\theta \cos\left(\frac{g_1 g_2 \mu_B^2}{\hbar}\frac{1}{r^3}(1 - 3\cos^2\theta)T\right). \tag{6}$$

$F(\nu)$ is a frequency-domain PELDOR lineshape, which is called dipolar Pake (resonance pattern) spectrum. Note that from Eq. (3) it follows that $F(\nu)$ is also normalized, $\int_{-\infty}^{\infty} F(\nu)d\nu = 1$.

Eq. (5) is also a first-kind Fredholm integral equation over $P(r)$, with the $K(\nu, r)$ as a kernel. To find $P(r)$, Eqs. (2) and (5) both may be equally used. But for the approach employed here, Eq. (5) is preferable. First, from the experimentally-obtained Pake spectrum direct assessment is possible of the distance interval, from r_{min} to r_{max}, in which $P(r)$ has significant

values. Second, the kernel (6) has a singularity at the frequency of $\nu = \frac{g_1 g_2 \mu_B^2}{2\pi\hbar}\frac{1}{r^3}$ which can essentially accelerate the convergence of the Monte Carlo process. For nitroxides this frequency may be approximately presented as $\frac{52\ \mathrm{MHz}}{(r/\mathrm{nm})^3}$. Third, the artefacts appearing because of intervention of electron-nuclear envelope modulation (ESEEM) can be simply avoided, because they produce peaks at the known frequencies.

3. Implementation

The suggested approach consists of the following steps.

(i) From the experimentally obtained $F(\nu)$ Pake spectrum, r_{min} and r_{max} distances are evaluated between which the $P(r)$ function has significant values. It can be done from the relations $r_{\min(\max)}/\mathrm{nm} = (52\ \mathrm{MHz}/\nu_{\max(\min)})^{1/3}$, where $\nu_{\max}$ is the high-frequency boundary of the Pake spectrum, and $\nu_{\min}$ is taken slightly below the low-frequency maximum of the spectrum.

(ii) The interval between r_{min} and r_{max} is divided into N subintervals, Δr_i. Here, we employed equal subintervals $\Delta r = (r_{max} - r_{min})/N$ (in principle, it is not necessary in a general case). So subintervals lie within the boundaries $r_i = r_{\min} + i\Delta r$, where $i = 0, 1, \ldots N$.

(iii) The trial distance distribution function, $P_{trial}(r_i)$, is constructed in the way that $P_{trial}(r_i) = 0$ for $i = 0$ and $i = N$; and that for other i numbers it is set to be a random ξ_i values distributed with equal probability between 0 and 1. Then, normalization in line with Eq. (3) is done using numerical integration employing the composite Simpson's rule (N is assumed to be an even number).

(iv) For the constructed $P_{trial}(r_i)$ function, the trial Pake spectrum $F_{trial}(\nu)$ is calculated by numerical integration of Eq. (5). Integration is performed employing also the composite Simpson's rule. It is done for a set of ν_j, $j = 1,2,\ldots J$, values (J is normally between 20 and 40) lying within the Pake spectrum.

(v) The mean-squared deviations (MSD), $\mathrm{MSD} = \sum_{j=1}^{J} C_j (F_{trial}(\nu_j) - F(\nu_j))^2 / \sum_{j=1}^{J} C_j$, between the calculated $F_{trial}(\nu_j)$ and the experimental $F(\nu_j)$ values are determined, where C_j are the weighting factors. Different trials are compared and the distribution $P_{trial}(r_i)$ providing the smallest MSD value is selected as a solution. Initially, weighting factors C_j are taken equal and then in some cases were selectively corrected depending on the obtained agreement between $F_{trial}(\nu_j)$ and $F(\nu_j)$ in the particular ν_j values. (In most cases described below this correction was unnecessary).

For broad distance distributions, when the distribution width is remarkably larger than Δr, the ξ_i values in step (iii) may be replaced by their modified ξ_i' values, obtained by a 3-point averaging of the adjacent values, $\xi_i' = (\xi_{i-1} + 2\xi_i + \xi_{i+1})/4$. This replacement means an effective increase of the distance discretization length (approximately by a factor of two); it may be employed selectively for different $i = 1,...N-1$ points. The necessity of this modification is determined empirically from agreement of simulated and experimental dipolar Pake spectra and the convergence rate of the Monte Carlo trials. The most appropriate N value is also assessed empirically.

Calculations were done on standard PC using common Pascal software (the PascalABC.NET version). Normally, number M of the trials were between 10^7 and 10^9. For $M = 10^7$, calculations took typically 1 – 2 min.

4. Results and Discussion

4.1. Two broad Gaussian distributions

To illustrate how the algorithm works, the model distance distribution function consisting of two Gaussian lines of unequal amplitude,

$$P(r) = a\frac{1}{\sqrt{2\pi}\delta_1}\exp\left(-\frac{(r-R_1)^2}{2\delta_1^2}\right) + (1-a)\frac{1}{\sqrt{2\pi}\delta_2}\exp\left(-\frac{(r-R_2)^2}{2\delta_2^2}\right), \quad (7)$$

was used, with the parameters $a = 0.7$, $R_1 = 2\,\text{nm}$, $R_2 = 3\,\text{nm}$, $\delta_1 = \delta_2 = 0.3\,\text{nm}$.

Results are presented in Fig. 1. The "experimental" $f(t)$ PELDOR signal time trace (Fig. 1a, it is given here only for illustrative purposes) and $F(\nu)$ Pake spectrum (Fig. 1b) were calculated using Eqs. (2) and (5), respectively. In the above algorithm of searching the best-fitted $P_{trial}(r_i)$ the minimal $r_{\min} \equiv r_0$ value was set to 1.2 nm, the maximal $r_{\max} \equiv r_N$ value was set to 3.7 nm; these boundaries correspond to the frequencies $\dfrac{52\,\text{MHz}}{(r_{\min(\max)}/\text{nm})^3}$ shown by arrows in Fig. 1b. In these calculations, three-point averaging for random trials, $\xi_i' = (\xi_{i-1} + 2\xi_i + \xi_{i+1})/4$, (see above) was employed.

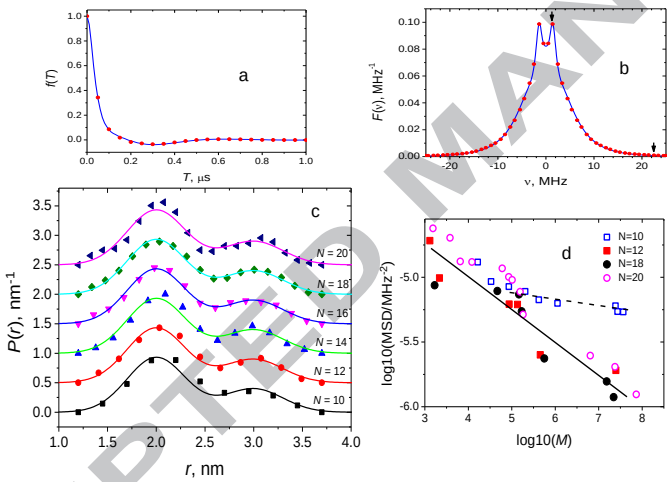

Fig. 1. Results of implementation of the described algorithm to the bimodal Gaussian distance distribution (7), with $a = 0.7$, $R_1 = 2\,\text{nm}$, $R_2 = 3\,\text{nm}$, $\delta_1 = \delta_2 = 0.3\,\text{nm}$. (a) Calculated PELDOR time traces: original data (blue solid line) and result of the fitting for N =16 (red circles). (b) The same for Pake spectrum; the arrows show the frequency positions corresponding to the largest and smallest distance with non-zero $P(r)$ values in the fitting. (c) the $P(r_i)$ distance distribution functions (symbols), obtained for different N, compared with the original one (solid lines); data are shifted along the vertical axis for convenience; (d) logarithmic plot of MSD between the set of true $F(\nu_j)$ spectral intensities and those best-fitted, as a function of number of trials M, for different N indicated. Solid line shows that MSD (for N = 12 and N = 18) is approximately proportional to $M^{-0.25}$.

The obtained best-fitted $P_{trial}(r_i)$ distributions are given in Fig. 1c, along with the original function (7). One can see that for small N value, N = 10, the calculated $P(r_i)$ function does not describe well the original function (7): the left maximum is shifted and the right maximum is not resolved. This disagreement can be readily explained as a consequence of the crudeness of numerical integration in Eq. (5), because the integration step is too large. For N values between 12 and 18 the calculated $P(r_i)$ are close to the original one. And for large N value (N = 20) the calculated $P(r_i)$ function starts to deviate; for N > 20 (data not shown) the deviation becomes remarkably larger. This deviation for large N can be attributed to the instability induced by the ill-posed nature of the integral equation (5), when different $P(r_i)$ solutions provide similar calculated $F(\nu)$ functions.

The MSDs for calculated and original $F(\nu_j)$ functions obtained for frequency points used in calculations (j = 1, … 40) are given in Fig. 1d as a function of number M of trials. The point positions along the horizontal axis is determined by selection of the accidentally achieved minimal MSD values. One can see that for N = 12 and N = 18, solid line drawn in Fig. 1b shows that MSD is approximately proportional to $M^{-0.25}$. MSDs for N = 10 are remarkably larger than those for larger N, which is an obvious consequence of the crudeness of integration mentioned above. This crudeness prevents good agreement with true Pake spectrum. So the convergence rate could serve as a marker of crudeness of integration.

We conclude from these model calculations that, fortunately, there exists a rather large intermediate interval (N is varying between 12 and 18), in which the solution is stable and describes satisfactorily the experimental results. In practical applications, when distribution is unknown, N should also be varied to meet two criteria that calculated and experimental spectra satisfactorily coincide and that the solution remain stable.

4.2. Two narrow Gaussian distributions

The distribution function given by Eq. (7) was also used with the same parameters except for the twice smaller widths, $\delta_1 = \delta_2 = 0.15$ nm. This is the case when two distances are well separated. Results of Monte Carlo fitting are shown in Fig. 2 for N = 28. It was found that algorithm does not work properly for small $P(r_i)$ values; so the $P(r_i)$ values were artificially set to zero for four r_i distance points between the two maxima (see Fig. 2c). Note that such artificial assignment would not make problem in the case of real experiment, when distance distribution is unknown – because the presence of separated maxima in distance distribution could be readily seen from presence of separated peaks in the Pake spectrum. Also, to achieve better agreement with the original Pake spectrum, weighting coefficients C_j were enhanced in the vicinity of the spectral shoulders at ± 5 MHz.

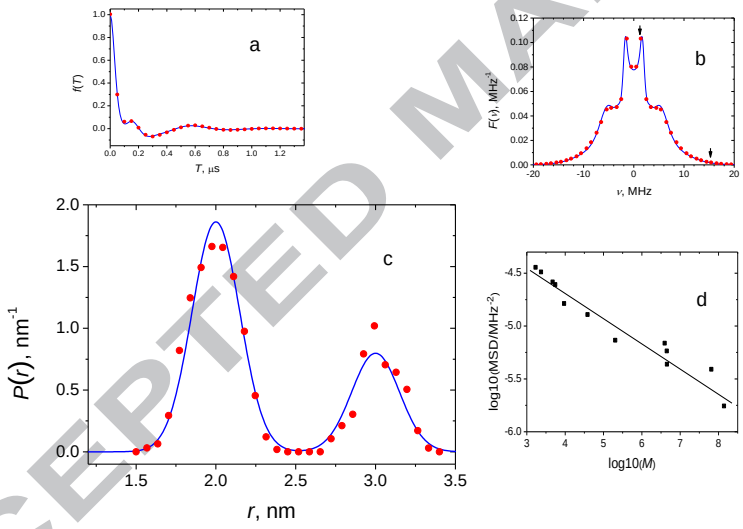

Fig. 2. The same as in Fig. 1, for δ twice smaller and N = 28. Solid line in (d) shows that MSD is proportional to $M^{-0.23}$. See text for other details.

4.3. The overlapping of narrow and broad Gaussian distributions

In these calculations, the distribution function given by Eq. (7) was used with the set of parameters: $a = 0.2$, $R_1 = 3$ nm, $R_2 = 3.5$ nm, $\delta_1 = 0.15$ nm, $\delta_2 = 1$ nm. This is the case of overlapping of narrow and broad distributions. Normally, PELDOR experiments deal with

distances larger than 1.5 nm, so this model $P(r)$ function was set to zero at distances $r < 1.5$ nm and multiplied correspondingly by a factor of 1.018 to match the normalization given by Eq. (3).

In this case, it would be reasonable if the distance discretization is different for the narrow and broad distance distributions. This goal could be achieved in different ways: simply by varying Δr_i with i number or by the 3-point averaging of the adjacent points, employed only for the distances outside the narrow distribution. As it was mentioned above, this averaging corresponds to effective increase of the discretization length Δr_i. Here, we employed the latter approach. It was found that for better agreement of original and calculated Pake spectra, this averaging should be done twice.

The results are shown in Fig. 3. Note that position of the narrow distribution at 3 nm can be simply evaluated *a priori* from the shoulder at the Pake spectrum at ± 1.9 MHz (see Fig. 3b). In Figs. 3a, 3b and 3c one can see a reasonable agreement of calculated results with the true data. Note that the rate of convergence given by data in Fig. 3d is noticeably slower (MSD is proportional to $M^{-0.09}$) than in the two previous cases. This may be explained by a crudeness of the integration step Δr for the narrow distance distribution, like it was suggested above in the subsection 4.1. (Certainly, the convergence can be further improved by using remarkably different Δr values for different distance ranges.)

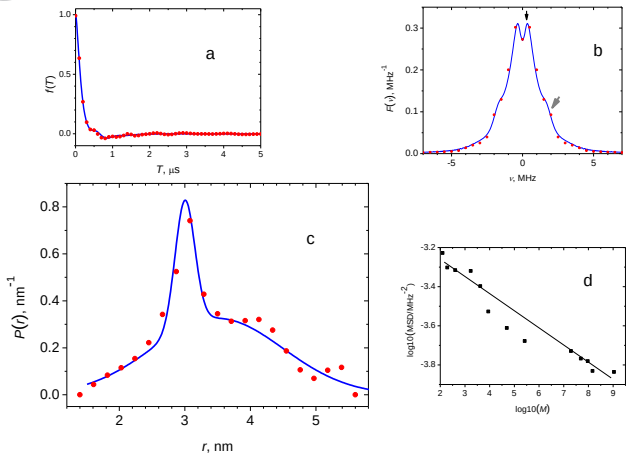

Fig. 3. The same as in Fig. 1, for the set of parameters: $a = 0.2$, $R_1 = 3\,\text{nm}$, $R_2 = 3.5\,\text{nm}$, $\delta_1 = 0.15\,\text{nm}$, $\delta_2 = 1\,\text{nm}$, and N =20. In (b), the arrow showing the frequency corresponding to the smallest distance with non-zero $P(r)$ values (12.7 MHz) is beyond the scale of the plot; and the inclined gray arrow indicates the shoulder corresponding to the narrow distance distribution. Solid line in (d) shows that MSD is proportional to $M^{-0.09}$. See text for other details.

The approach used here when for different distance ranges different regularization lengths are used may be called as selective regularization. The possibility of such selectivity may be considered as an obvious advantage of the technique as compared with those using Tikhonov regularization.

4.4. Doubly spin-labelled 13-mer of DNA

In [22], PELDOR experiments were done on the doubly spin-labeled 13-mer of DNA duplex:

5' TpCpTpCpTpCpGpCpCpTpTpCpC 3'

3' **R**-ApGpApGpApGpCpGpGpApApGpG-**R** 5',

where **R** denotes the nitroxide spin label. In these studies, deuterated water/glycerol mixture (1:1 v/v) was used as a solvent.

In Fig. 4, the original $V_N(T)$ time trace obtained from data [22] is given along with its Fourier transform and results of implementation of the described Monte Carlo algorithm. It was found that the peculiarities seen in the central part of the spectrum (see Fig. 4b) can be described only if a small admixture of $P(r)$ at long distances is added. We used here a model $P(r)$ function

linearly diminishing with r increasing above 6.5 nm (see Fig. 4c). Probably this admixture in experiments [22] is induced by presence of a small amount of single-stranded DNAs.

In Fig. 4c, results of calculations [22] obtained using common approach based on Tikhonov regularization also are presented. One can see that the approach used here provides very similar information.

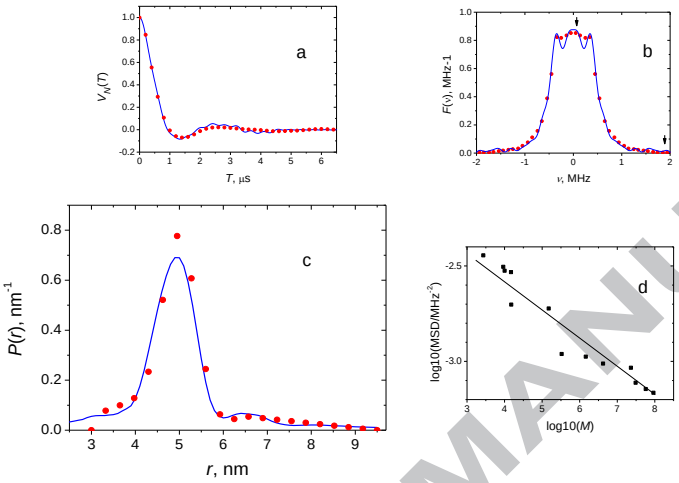

Fig. 4. Results of implementation of the described algorithm for PELDOR data obtained in [22] for doubly spin-labeled DNA in frozen deuterated water/glycerol mixture. The meanings of the presented data are the same as in Fig. 1. In (c), the fitted distance distribution function (red circles) is compared with that found in [22] where it was obtained with Tikhonov regularization (solid blue line). Solid line in (d) shows that MSD is proportional to $M^{-0.16}$. See text for other details.

4.5. Peptide antibiotic ampullosporin A

Doubly spin-labeled peptide antibiotic ampullosporin A having the amino acid sequence

Ac-Trp-Ala-**R**-Aib-Leu-Aib-Gln-Aib-Aib-Aib-Gln-Leu-**R**-Gln-Lol,

was studied in [20]. Here, **R** is a spin-labeled amino-acid. In [20], the obtained experimental PELDOR data were treated by the preliminary version of the algorithm suggested here. Here we treat these data in more detail (Δr here is much smaller than that used in [20]).

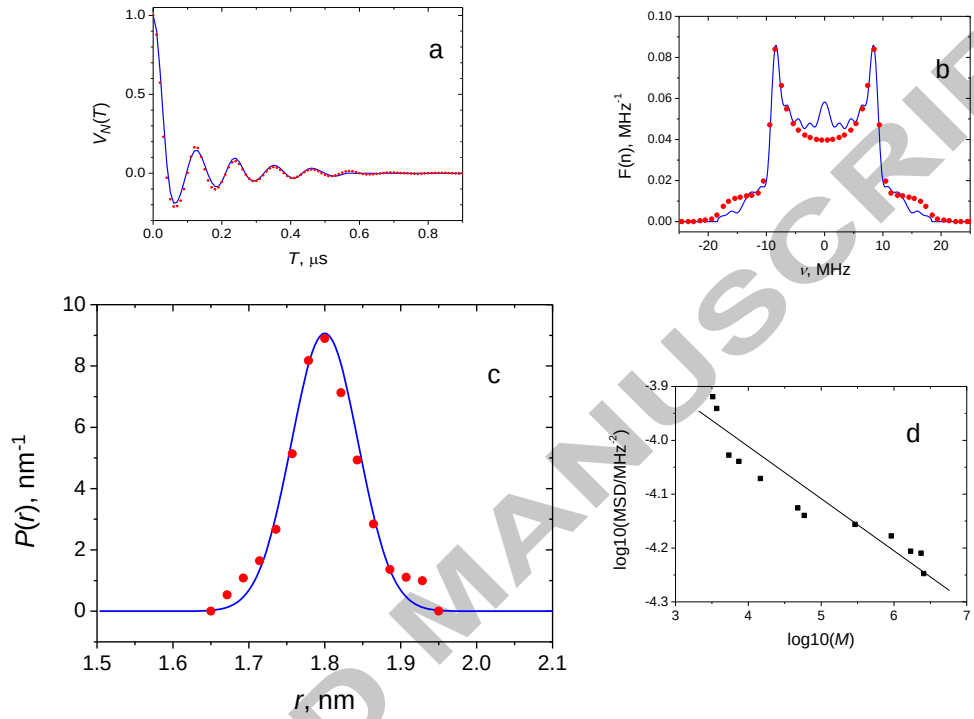

Fig. 5. Results of implementation of the described algorithm for PELDOR data obtained in [20] for doubly spin-labeled ampullosporin A in frozen methanol solution. The meanings of the presented data are the same as in Fig. 1. Solid blue line in (c) presents result of calculations taken from literature [23], which were obtained using Tikhonov regularization for the same system. Solid line in (d) shows that MSD is proportional to $M^{-0.27}$.

Fig. 5 presents original PELDOR $V_N(T)$ data for spin-labeled ampullosporin A in frozen methanol solution, its Fourier transform – the Pake resonance spectrum, results of implementation of the described Monte Carlo algorithm, along with the results [23] in which common approach based on the Tikhonov regularization algorithm was employed perfectly for the same system. From the results shown in Fig. 5c, one can see that the approach employing

Tikhonov regularization [23] and the suggested Monte Carlo approach provide very similar results.

5. Conclusions

It is shown that solution of integral equation for deriving distance distribution from the experimental PELDOR data can be stabilized by increasing the distance discretization length Δr. The solution is stabilized because numerical integration at large Δr strongly depends on the smoothness of the function under integral. From the other side, Δr must be not so large that integration becomes inaccurate. Fortunately, the intermediate region exists in which the Δr is not so small that the instability appears and Δr is not so large that integration remains reasonably accurate. For most commonly occurring experimental situations, the number of discretization intervals between 10 and 20 – 30 (depending on the shape of distance distribution) serves well to meet these opposite requirements.

Solving the integral equation may be performed using Monte Carlo trials of the distance distribution function. This approach allows to fulfill automatically the constrain of non-negativity of $P(r_i)$. As the number of discretization intervals is not high and the kernel of integral equation possesses a singularity, the Monte Carlo process converges reasonably rapidly. In the case of admixing of low-intensity distance distributions, the $P(r_i)$ values for these admixtures should be replaced by an appropriate model function.

In the case of overlapping of narrow and broad lines, it is shown here that a selective distance discretization is helpful when for different distance ranges different regularization lengths are used. The possibility of such selectivity may be considered as an advantage, as compared with the techniques using Tikhonov regularization. In simple cases, the obtained results of determination of distance distribution from experimental PELDOR data on spin-labeled biomolecules show good agreement with those obtained by traditional Tikhonov

regularization approach. So the suggested approach could serve as a useful complement to the traditional methods.

Acknowledgements

Author thanks Maxim Yurkin for helpful discussion and Gunnar Jeschke for useful suggestions. This work was supported by the Russian Science Foundation, grant # 15-15-00021.

References

[1] A.D. Milov, K.M. Salikhov, M.D. Schirov, Application of ELDOR in electron spin echo for paramagnetic center space distribution in solids, Fiz. Tverd. Tela (Leningrad) 23 (1981) 975–982.

[2] A.D. Milov, A.B. Ponomarev, Y.D. Tsvetkov, Electron-electron double resonance in electron spin echo: Model biradical systems and the sensitized photolysis of decalin, Chem. Phys. Letters 110 (1984) 67–72.

[3] O. Schiemann, T.F. Prisner, Long-range distance determinations in biomacromolecules by EPR spectroscopy, Quart. Rev. Biophys. 40 (2007) 1–53.

[4] A. Savitsky, K. Möbius, High-field EPR, Photosynth. Res. 102 (2009) 311–333.

[5] J.P. Klare, H.-J. Steinhoff, Spin labeling EPR, Photosynth. Res. 102 (2009) 377-390.

[6] G.W. Reginsson, O. Schiemann, Pulsed electron-electron double resonance: Beyond nanometre distance measurements on biomacromolecules Biochem. J. 434 (2011) 353-363.

[7] G. Jeschke, DEER distance measurements on proteins, Ann. Rev. Phys. Chem. 63 (2012) 419–446.

[8] D. Goldfarb, Gd^{3+} spin labeling for distance measurements by pulse EPR spectroscopy Phys. Chem. Chem. Phys. 16 (2014) 9685-9699.

[9] T.F. Prisner, A. Marko, S.Th. Sigurdsson, Conformational dynamics of nucleic acid molecules studied by PELDOR spectroscopy with rigid spin labels, J. Magn. Reson. 252 (2015) 187–198.

[10] A.D. Milov, Y.D. Tsvetkov, J. Raap, M. De Zotti, F. Formaggio, C. Toniolo, Conformation, self-aggregation, and membrane interaction of peptaibols as studied by pulsed electron double resonance (PELDOR) spectroscopy, Biopolym. 106 (2016) 6–24.

[11] G. Jeschke, A. Koch, U. Jonas, A. Godt, Direct conversion of EPR dipolar time evolution data to distance distributions, J. Magn. Reson. 155 (2002) 72-82.

[12] A.D. Milov, Y.D. Tsvetkov, F. Formaggio, S. Oancea, C. Toniolo, J. Raap, Solvent effect on the distance distribution between spin labels in aggregated spin labeled trichogin GA IV dimer peptides as studied by pulsed electron-electron double resonance, Phys. Chem. Chem. Phys. 6 (2004) 3596-3603.

[13] M.K. Bowman, A.G. Maryasov, N. Kim, V.J. DeRose, Visualization of distance distribution from pulsed double electron-electron resonance data, Appl. Magn. Reson. 26 (2004) 23-39.

[14] G. Jeschke, G. Panek, A. Godt, A. Bender, H. Paulsen, Data analysis procedures for pulse ELDOR measurements of broad distance distributions, Appl. Magn. Reson. 26 (2004) 223-244.

[15] G. Jeschke, A. Bender, H. Paulsen, H. Zimmermann, A. Godt, Sensitivity enhancement in pulse EPR distance measurements, J. Magn. Reson. 169 (2004) 1-12.

[16] W.-Y. Chiang, P.P. Borbat, J.H. Freed, The determination of pair distributions by pulsed ESR using Tikhonov regularization, J. Magn. Reson. 172 (2005) 279-295.

[17] W.-Y. Chiang, P.P. Borbat, J.H. Freed, Maximum entropy: a complement to Tikhonov regularization for determination of pair distance distributions by pulsed ESR, J. Magn. Reson. 177 (2005) 184-196.

[18] G. Jeschke, V. Chechik, P. Ionita, A. Godt, H. Zimmermann, J . Banham, C. R. Timmel, D. Hilger, H. Jung, DeerAnalysis2006 - a comprehensive software package for analyzing pulsed ELDOR data, Appl. Magn. Reson. 30, 473-498 (2006)

[19] S. Brandon, A.H. Beth, E.J. Hustedt, The global analysis of DEER data (2012) J. Magn. Reson. 218 (2012) 93-104.

[20] V.N. Syryamina, R.I. Samoilova, Y.D. Tsvetkov, A.V. Ischenko, M. De Zotti, M. Gobbo, C. Toniolo, F. Formaggio, S.A. Dzuba, Peptides on the surface: spin-label EPR and

PELDOR study of adsorption of the antimicrobial peptides Trichogin GA IV and ampullosporin a on the silica nanoparticles, Appl. Magn. Reson. 47 (2016) 309-320.

[21] K.M. Salikhov, I.T. Khairuzhdinov, R. B. Zaripov, Three-pulse ELDOR theory revisited, Appl. Magn. Reson. 45 (2014) 573–619.

[22] N.A. Kuznetsov, A.D. Milov, N.P. Isaev, Yu.N. Vorobjev, V.V.Koval, S.A. Dzuba, O.S. Fedorova, Y.D. Tsvetkov, PELDOR analysis of enzyme-induced structural changes in damaged DNA duplexes, Mol. BioSyst. 7 (2011) 2670–2680.

[23] A.D. Milov, Yu.D. Tsvetkov, M. Bortolus, A.L. Maniero, M. Gobbo, C. Toniolo, F. Formaggio. Synthesis and conformational properties of a TOAC doubly spin-labeled analog of the medium-length, membrane-active peptaibiotic ampullosporin A as revealed by CD, fluorescence, and EPR spectroscopies, Biopolym. 102 (2014) 40-48.

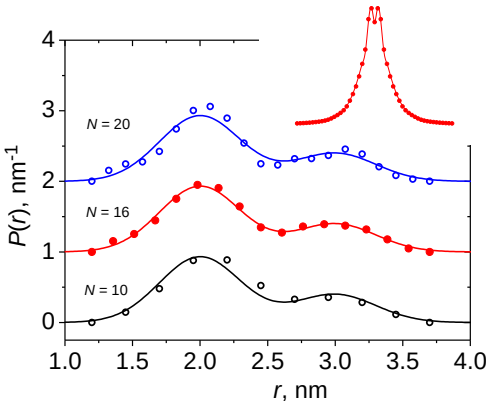

Graphical abstract